

Astrophysical deductions from the quasi-steady-state cosmology

F. Hoyle,¹ G. Burbidge² and J. V. Narlikar³

¹102 Admirals Walk, Bournemouth, Dorset BH2 5HF

²Center for Astrophysics and Space Sciences and Department of Physics, University of California, San Diego, La Jolla, CA 92093-0111, USA

³Inter-University Centre for Astronomy and Astrophysics, Post Bag 4, Ganeshkind, Pune 411 007, India

Accepted 1993 November 24. Received 1993 November 23; in original form 1993 June 10

ABSTRACT

The numerical consequences of the theory developed in two previous papers are examined in more detail. In particular, it is shown that the radio source count data can be explained to high accuracy, including the steeper-than-Euclidean slope of the count distribution at its high-flux end. By specifying the parameters of the theory, we obtain reasonable values for the Hubble constant and the ages of the globular clusters, a maximum redshift for any object observed from the present oscillatory cycle of the Universe, a minimum average density of $\sim 2 \times 10^{-27} \text{ g cm}^{-3}$ for clusters of galaxies, and a temperature close to 2.7 K for the microwave background. The theory predicts a near-blackbody spectrum for the microwave background, and also explains the observed anisotropy.

Key words: cosmic microwave background – cosmology: observations – cosmology: theory – large-scale structure of Universe.

1 INTRODUCTION

In two previous papers (Hoyle, Burbidge & Narlikar 1993, 1994, referred to as HBN I and II), we have developed a new model for the Universe based on matter creation, which we have called quasi-steady-state cosmology (QSSC). The Robertson–Walker form of the space–time metric of the theory is

$$ds^2 = dt^2 - \frac{S^2(t)}{S^2(t_0)} [dr^2 + r^2(d\theta^2 + \sin^2\theta d\varphi^2)], \quad (1)$$

in which $t = t_0$ is the present moment of time and

$$S(t) = \exp \frac{t}{P} \left(1 + \alpha \cos \frac{2\pi t}{Q} \right), \quad (2)$$

with $P \gg Q$ and $0 < \alpha < 1$. The theory therefore has four parameters: α , P and Q , and t_0 which decides the phase of the present moment with respect to the oscillatory factor in (2). In HBN II the parameters were broadly specified. Here we shall be more precise about the specification.

2 THE VALUES OF THE PARAMETERS OF THE THEORY

It is possible in principle to infer the values of the parameters of the theory from astrophysically determined quantities. Unfortunately, however, certain of the latter do not have

values that are generally agreed among astronomers. It is necessary therefore to invert the situation, by specifying the parameters and then working out the consequent astrophysical quantities.

The zero of time, $t = 0$, has been chosen to be at an oscillatory maximum, which we further particularize as the last maximum to occur before the present epoch at $t = t_0$. It will be useful to employ a number of semantic expressions, defined as follows:

‘present half-cycle’	$\equiv 0.5Q \leq t \leq t_0$,
‘previous half-cycle’	$\equiv 0 \leq t \leq 0.5Q$,
‘present cycle’	$\equiv 0 \leq t \leq t_0$,
‘previous cycle’	$\equiv -Q \leq t \leq 0$,
‘earlier cycles’	$\equiv t \leq -Q$.

It will often be convenient to use Q as the unit of t .

Leaving P to be determined at a later stage, our parameter choices are

$$\alpha = 0.75, \quad t_0 = 0.85Q, \quad Q = 4.0 \times 10^9 \text{ yr}. \quad (3)$$

The time since the last minimum of $S(t)$ is then 14×10^9 yr. Since the creation of matter is mostly associated with the oscillatory minima, it is natural to regard the minima as epochs of star formation. Most star clusters will also be associated with the minima, those formed at the last minimum having ages of about 14×10^9 yr, those at the previous minimum 54×10^9 yr, and so on. Of these, it will be clusters

of age 14×10^9 yr that dominate the astrophysical situation, since stars in a cluster of age 54×10^9 yr or more would be burned out down to very low main-sequence luminosities and could not be distinguished in the detail required to construct the colour-magnitude diagrams from which age estimates are made.

Since the factor $\exp(t/P)$ in (2) is effectively unity throughout the present cycle, the largest possible redshift from the present cycle is given to a good approximation by

$$4(1 + 0.75 \cos 1.7\pi) - 1 = 4.76. \quad (4)$$

As is shown later, when the factor $\exp(t/P)$ is included, this redshift is increased to 4.86. We shall also show that the corresponding redshift of objects from the previous cycle is 5.166, and so on step by step to still larger redshifts from earlier minima, with the objects in each cycle being fainter than those in the most recent cycle by about 3 mag.

With the speed of light equal to unity, Hubble's constant is given by

$$H_0 = \left(\frac{\dot{S}}{S} \right)_{t=t_0} = - \frac{1.5\pi \sin 1.7\pi}{1 + 0.75 \cos 1.7\pi} = 2.646, \quad (5)$$

the unit of time being Q , or, in conventional units with $Q = 4 \times 10^{10}$ yr,

$$H_0 = \frac{2.646}{Q} = 64.7 \text{ km s}^{-1} \text{ Mpc}^{-1}. \quad (6)$$

Also, by definition,

$$q_0 = \left(\frac{-S\dot{S}}{S^2} \right)_{t=t_0} = \frac{\cos 1.7\pi(1 + 0.75 \cos 1.7\pi)}{0.75 \sin^2 1.7\pi} = 1.725. \quad (7)$$

The best value for q_0 obtained by Kristian, Sandage & Westphal (1978) and Sandage (private communication), from a comparison of curves predicted by Friedmann models with observed points for galaxies in a redshift-magnitude plot, was 1.5. However, the curves in such a diagram given by the present theory for various values of q_0 are not the same as in the Friedmann models, and so it is necessary to postpone this issue for discussion at a later stage.

Without altering α and t_0 from the values given in (3) by amounts that seem otherwise unacceptable, the value of H_0 cannot be changed much by seeking to raise or lower the number 2.646 in (4). A change in Q , however, will lead to another value for H_0 . Thus if we put $Q = 3 \times 10^{10}$ yr then $H_0 = 86.2 \text{ km s}^{-1} \text{ Mpc}^{-1}$, while if $Q = 5 \times 10^{10}$ yr, then $H_0 = 51.7 \text{ km s}^{-1} \text{ Mpc}^{-1}$. In the former case, however, the globular cluster ages would be only 10.5×10^9 yr, which seems too small, and there is a time problem similar to that in the Friedmann models. With $Q = 5 \times 10^{10}$ yr and $H_0 = 51.7 \text{ km s}^{-1} \text{ Mpc}^{-1}$, however, the globular cluster ages are 17.5×10^9 yr, which from the point of view of stellar structure theory seems optimum. An age of 17.5×10^9 yr also agrees very well with that of the r -process elemental ages determined by Clayton (1988) using the osmium/rhenium chronometer, but there is then some discrepancy with the age of about 12×10^9 yr for the r -process elements first determined by Fowler & Hoyle (1960) and more recently by Fowler (1987). For a more detailed discussion of the radioactive age determinations, see Cowan, Thielemann & Truran

(1991). The problems are largely avoided here by an intermediate choice for Q , namely $Q = 4 \times 10^{10}$ yr in (3).

3 RELATIONS BETWEEN t , z AND r FOR LIGHT TRACKS

The coordinate r is taken to be zero for the observer. For radiation emitted at time t and received at t_0 , the radial coordinate associated with the emitting object is given by

$$r = S(t_0) \int_t^{t_0} \frac{dt}{S(t)}, \quad (8)$$

and the redshift z associated with the radiation by

$$1 + z = \frac{S(t_0)}{S(t)} = \frac{1 + \alpha \cos 2\pi t_0}{1 + \alpha \cos 2\pi t}. \quad (9)$$

We shall study these relations first for the case in which the time difference $(t_0 - t)$ is of order Q . For $P \gg Q$ we can approximate $\exp(t - t_0)/P$ by unity. Then when $S(t) \approx 1 + \alpha \cos 2\pi t$, t being in units of Q , (8) becomes

$$r = (1 + \alpha \cos 2\pi t_0) \int_t^{t_0} \frac{dt}{1 + \alpha \cos 2\pi t}, \quad (10)$$

which integrates to give

$$r = \frac{1 + \alpha \cos 2\pi t_0}{\pi \sqrt{1 - \alpha^2}} \left[\tan^{-1} \left(\frac{1 - \alpha}{\sqrt{1 - \alpha^2}} \tan \pi t \right) \right]_t^{t_0}. \quad (11)$$

Using $\alpha = 0.75$ and $t_0 = 0.85$ from (3), Table 1 gives values of z , r and F calculated for a number of times t in the present half-cycle of $S(t)$. Here, F is defined by

$$F = \frac{1}{r^2(1 + z)^2}. \quad (12)$$

This quantity varies as the bolometric flux from sources at different r but otherwise intrinsically the same. These values can also be used for fluxes through a restricted bandwidth, provided that the sources have logarithmic spectra, $d\nu/\nu$.

Reckoning cycles from one minimum of $S(t)$ to the next, in Table 2 we give values of z , r and F for the previous cycle.

The apparent bolometric magnitude m of a galaxy of intrinsic magnitude M is given at various values of r by

$$m = M + 5 \log \left(\frac{cQ}{3.08 \times 10^{19}} \right) + 5 \log(1 + z) + 5 \log r + \Delta, \quad (13)$$

in which the redshift z is related to r by the values given in Tables 1 and 2. Here, Δ is the extinction produced by intergalactic material in the passage of light from the galaxy to the observer. With the choice in (3) of $Q = 40 \times 10^9$ yr and for a galaxy of intrinsic magnitude -22.44 we thus obtain

$$m = 23 + 5 \log(1 + z) + 5 \log r + \Delta. \quad (14)$$

It is usual to suppose that $\Delta = 0$ for galaxies observed optically, and this we take to be the case for values of r belonging to the present half-cycle of the oscillations of $S(t)$. For galaxies observed from the previous half-cycle, however,

Table 1. Values of z , r and F for values of t in the present half-cycle of $S(t)$.*

t	z	r	F	$z^2 F$
.85	-	-	-	-
.84	.028	.0101	9204.	7.377
.83	.059	.0206	2106.	7.451
.82	.094	.0313	852.4	7.490
.81	.131	.0424	434.2	7.493
.80	.173	.0539	250.2	7.460
.78	.268	.0782	101.7	7.291
.76	.382	.1046	47.87	6.994
.74	.520	.1334	24.31	6.582
.72	.687	.1652	12.86	6.078
.70	.890	.2007	6.953	5.503
.68	1.135	.2405	3.792	4.884
.66	1.432	.2857	2.071	4.247
.64	1.790	.3373	1.129	3.618
.62	2.216	.3966	.6150	3.019
.60	2.710	.4649	.3361	2.469
.58	3.261	.5435	.1865	1.983
.56	3.830	.6332	.1069	1.568
.54	4.349	.7336	.06494	1.228
.52	4.724	.8429	.04296	0.959
.50	4.865	.9572	.03173	0.751

*Note that the values in this table for z include the factor $\exp(t/P)$ in equation (2) for $S(t)$, calculated for $P/Q=20$.

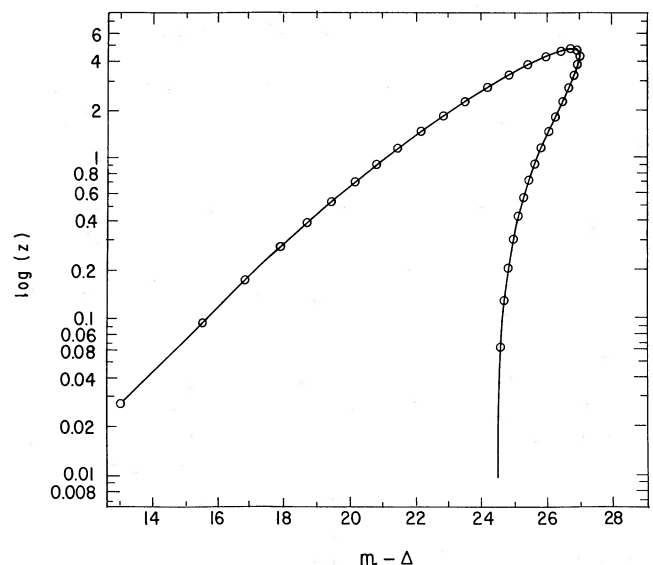
the light is required to have passed through the minimum at $t=0.5$, where the density of diffuse intergalactic absorbing material would be enhanced by $(1+z)^3 \approx 200$. This large increase suggests that a non-zero value of Δ would be appropriate when galaxies are observed optically from the previous half-cycle.

The Friedmann model with $q_0 = +1$ has flux F proportional to z^{-2} , i.e. the product $z^2 F$ is constant. The products in the last column of Table 1 show that the present model with $q_0 = 1.725$ does not behave at all like a Friedmann model. Rather, the situation is like the $q_0 = +1$ Friedmann model for redshifts < 1 , but thereafter in a redshift-magnitude diagram the calculated points go to the right, rather than to the left of the line for $z^2 F$ constant. Fig. 1 gives the plot of $(m - \Delta)$ versus $\log z$ for galaxies with $M = -22.44$. It is interesting that galaxies become brighter and bluer towards the last oscillatory maximum at $t=0$. The theory thus requires the existence of a very large number of faint blue galaxies with small redshifts or even small blueshifts.

The present-day average density in the Universe deduced from the well-known closure relationship, a form of which applies in the present theory, is $\sim 10^{-29} \text{ g cm}^{-3}$. At the last oscillatory minimum with $(1+z)^3 \approx 200$, this value would have been raised to $\sim 2 \times 10^{-27} \text{ g cm}^{-3}$, which is similar to the average densities found in many gravitationally bound clusters of galaxies. Since, at oscillatory minima, bound clusters cannot become like holes in a Swiss cheese, it follows that $\sim 2 \times 10^{-27} \text{ g cm}^{-3}$ must be a lower limit to the average densities in bound clusters, explaining why this value appears so frequently in the observations of clusters.

Table 2. Values of z , r and F for the previous cycle.

t	z	r	F
.47	4.578	1.127	.02530
.44	3.859	1.281	.02580
.41	3.016	1.412	.03111
.38	2.254	1.518	.04098
.35	1.642	1.604	.05569
.32	1.174	1.674	.07553
.29	.821	1.732	.1005
.26	.557	1.781	.1300
.23	.359	1.823	.1630
.20	.208	1.861	.1978
.18	.129	1.883	.2211
.16	.064	1.904	.2436
.14	.010	1.924	.2647
.12	-.0338	1.943	.2836
.10	-.0690	1.962	.2998
.08	-.0965	1.979	.3126
.06	-.1169	1.997	.3217
.04	-.1309	2.013	.3266
.02	-.1389	2.030	.3273
.00	-.1409	2.046	.3235
-.02	-.1371	2.063	.3156
-.04	-.1274	2.080	.3037
-.06	-.1116	2.096	.2883
-.08	-.0892	2.114	.2699
-.10	-.0596	2.131	.2490
-.12	-.0222	2.149	.2264
-.14	.0240	2.168	.2027
-.16	.081	2.188	.1787
-.18	.150	2.210	.1549
-.20	.233	2.232	.1320
-.23	.390	2.269	.1005
-.26	.598	2.312	.07325
-.29	.875	2.361	.05103
-.32	1.244	2.419	.03393
-.35	1.736	2.489	.02156
-.38	2.380	2.575	.01320
-.41	3.184	2.681	.007946
-.44	4.078	2.812	.004907
-.47	4.846	2.966	.003327
-.50	5.166	3.136	.002675

**Figure 1.** A plot of $\log z$ versus $(m - \Delta)$ for $M = -22.44$ (Section 3).

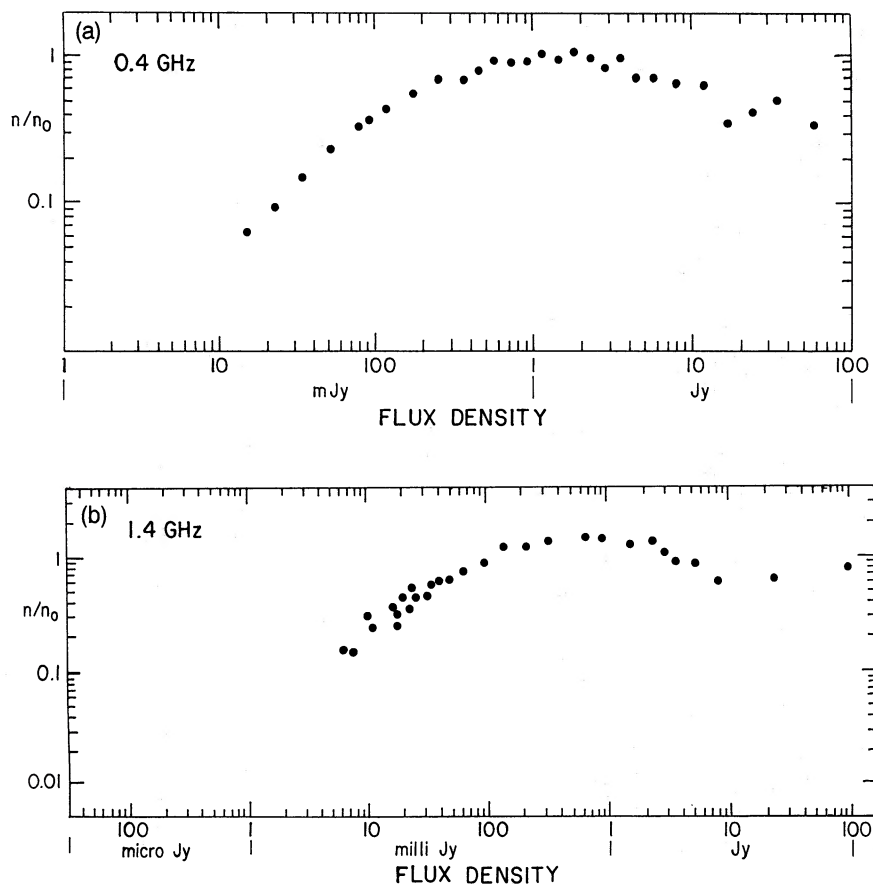


Figure 2. Counts of radio sources at 408 MHz and 1.4 GHz, with the latter restricted to flux values greater than $\sim 10^{-2}$ Jy, redrawn from Kellermann & Wall (1987). The counts are normalized to a uniformly filled static Euclidean universe (Section 4).

4 DEDUCTION OF THE RATIO P/Q FROM RADIO SOURCE COUNTS

The special feature of radio astronomy is that it provides observations that seem to go back to oscillations of $S(t)$ much earlier than the present and previous cycles. Radio astronomy appears capable of penetrating deeper into the Universe than at any other waveband, except possibly gamma-rays.

In big bang cosmology, attempts to explain the radio source counts are highly complicated, involving evolutionary hypotheses both with respect to the time dependence of the frequency of occurrence of sources and with respect to the behaviour of their luminosity function. Here we make no such complicated hypotheses. Rather, we take all sources to be similar to one another, and we consider their frequency of occurrence per unit proper spatial volume also to be a constant, the simplest possible assumptions. For those sources that occurred k cycles ago, i.e. over the time range $-k \leq t \leq -k+1$, it will be those that happened close to the ends of the range that dominate the count. This is because such sources have far higher apparent magnitudes than those that happened near the oscillatory minima at $t = -k+0.5$, as can be seen from the tabular values of F for the case $k=1$ in Table 2.

Taking F to be the flux from a standard source, we now write

$$F = \frac{\text{constant}}{r^2(1+z)^2}. \quad (15)$$

The brightest sources from the k th oscillatory cycle are those that occur near maximum phase, where the radial coordinate takes the value r_k , given approximately by

$$r_k \approx 2.18 k, \quad (16)$$

when k becomes appreciably larger than unity. The factor $(1+z)^{-2}$ in (15) varies with k as $\exp(-2k/P)$, so that the flux F_k from sources near maximum phase is given for the k th cycle by

$$F_k \approx \frac{\text{constant}}{k^2} \exp\left(-\frac{2k}{P}\right), \quad (17)$$

while the number N_k of sources back in time to the k th cycle is given by

$$N_k = \text{constant} \times r_k^3 \exp\left(-\frac{3k}{P}\right), \quad (18)$$

the exponential factor being required to convert coordinate volume to proper volume. Immediately, from (17) and (18) we have

$$N_k F_k^{3/2} = \text{constant} \times \exp\left(-\frac{6k}{P}\right). \quad (19)$$

It is usual to display integral source counts as a plot of $\log NF^{3/2}$ against $\log F$, obtained observationally by choosing a number of values of F and determining the number of sources brighter than F , each value chosen for F giving a point in the plot. Equations (17) and (19) give a set of theoretical points in such a plot, with $F = F_k$ for various k corresponding to the flux from the standard source at the maximum of the k th cycle. Were P very large, so as to make the exponential factors in (17) and (19) essentially unity for the values of k in question, we would have a set of points in a $\log NF^{3/2}$ - $\log F$ plot that were similar to points for sources in Euclidean space. Successive cycles would have a Euclidean relationship with respect to each other, a feature well known from observation and hitherto seen as a mysterious property of the counts. According to the value chosen for P , however, the exponential factor $\exp(-6k/P)$ in (19) produces a decline from the Euclidean level in the plot for k increasing sufficiently, and, by comparing this decline with that actually observed, it is possible to infer the value of P , and so the value of the remaining parameter in the theory. Since P is in units of Q , it is the ratio P/Q that is thus determined.

We are concerned with highly luminous sources, and for these the observations are best represented by relatively low-frequency surveys, at 408 MHz and 1.4 GHz, for which the data given by Kellermann & Wall (1987) are shown in Fig. 2. Because low-luminosity sources tend to dominate the counts increasingly at small values of F , only observations for $F > \sim 10^{-2}$ Jy are included in the plot for 1.4 GHz. The general features of the observations are evidently the same at the two frequencies, and are as follows:

- (1) an irregular situation at fluxes between 10 and 100 Jy;
- (2) a rise of level from 10 Jy down to ~ 2 Jy;
- (3) a high plateau maintained over range of about 10 in the flux F ;
- (4) an eventual fall-off by a factor ~ 10 as F declines to $\sim 10^{-2}$ Jy.

The above brief theoretical sketch is not sufficient to provide an adequate comparison with these observations. For this, theoretical predictions are needed at more general values of F , rather than just at oscillatory maxima, and a differential plot rather than an integral one is required. Using the computer program described in the Appendix, this has been done for a luminosity function going from 10^{29} to 10^{30} W Hz^{-1} , the explicit values of which yield the abscissa scale in Fig. 3 in Jy, a scale that can be compared with the observations at 408 MHz in Fig. 2. Numbers of sources are marked at several values of F relative to 100 at $F = 10$ Jy taken as standard. The number of sources becomes very small at the extreme right of both Figs 2 and 3, and so the points there are irregular, as expected.

The theoretical curve of Fig. 3 was calculated for $P/Q = 20$. A lesser value of P/Q would give a steeper fall-off of the points towards 10^{-2} Jy, while a larger value would give

a more gentle fall-off. Since the declines in Figs 2 and 3 towards low F match very well, this comparison of theory with observation will be taken to determine P/Q as being not much different from 20.

5 THE BRIGHT END OF THE DIAGRAM

Although the calculated curve of Fig. 3 is generally similar at the bright end to the data of Fig. 2, there are differences of detail that are worth examining. At the bright end, the data are dominated by local sources of lower luminosity than have been included in the theoretical curve, which is wholly for sources with $L \geq 10^{29}$ W Hz^{-1} at 408 MHz. At values of $F < 1$ Jy, these local sources become unimportant, however, and so they were irrelevant for the determination of P/Q in the preceding section. For the purpose of connecting sources from the present half-cycle with those of the previous cycle, however, it is necessary to remove them as far as possible from the data.

The 3CR catalogue contains 298 extragalactic sources observed over 4.05 sr. Obtained at a frequency of 178 MHz, it is considered complete for $F \geq 10$ Jy but not for F less than 10 Jy. Thus, in order to confine the discussion to a complete sample, it is necessary to remove those sources having $F < 10$ Jy. After also removing those that as yet have not been identified, usually for reasons of obscuration, 217 identified sources with $F \geq 10$ Jy remain. The great majority are readily classifiable from their measured fluxes and redshifts to have either $L \lesssim 10^{29}$ W Hz^{-1} or luminosities much less than this, with only a small fraction as borderline cases. We found the count to be 85 high-luminosity sources and 132 low-luminosity ones.

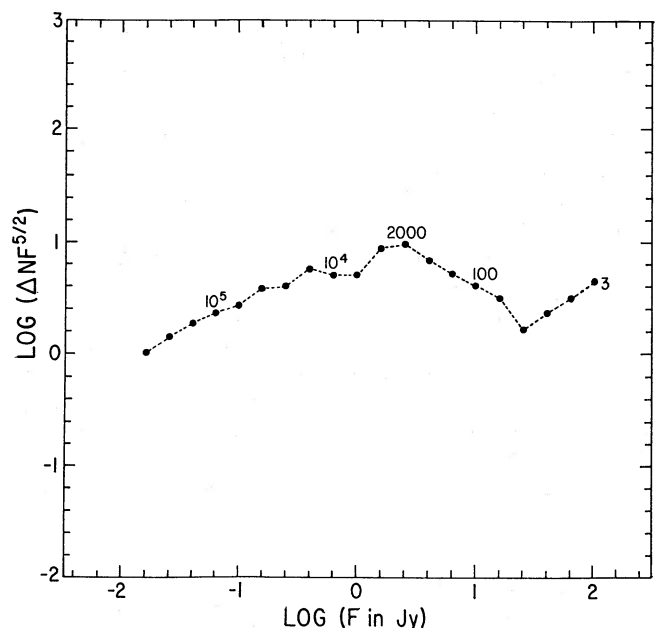


Figure 3. A plot of $\log(\Delta N F^{5/2})$ against $\log F$ for a luminosity function $L^{-2.1}$ extending from 10^{29} to 10^{30} W Hz^{-1} , the quantity ΔN being the number of sources counted in a small standard increment of $\log F$, the ordinate being in arbitrary units and the abscissa in Jy (Section 4).

According to Fig. 3, in going from $F = 10$ Jy down to the 4C threshold at $F = 2$ Jy, the high-luminosity sources rise by a factor of about 2.5 above the Euclidean expectation, i.e. by a factor of $2.5(5)^{3/2} = 28$, which is to say that the 85 high-luminosity sources at $F = 10$ Jy give a theoretical expectation of 2380 such sources at $F = 2$ Jy. The low-luminosity sources can rise at most by the Euclidean factor $5^{3/2} = 11.2$, i.e. at most from 132 to 1480. The expectation is therefore that high-luminosity sources are already dominant at $F = 2$ Jy, and still more so as F falls below 2 Jy. Thus the percentages expected for sources in the 4C catalogue with its threshold at 2 Jy are ~ 60 per cent for high luminosities and 40 per cent for low luminosities.

About half of the high-luminosity sources in the 3CR catalogue are radio galaxies and half are QSOs. With the same approximate equality down to $F = 2$ Jy, the percentages for the 4C catalogue are 30 per cent high-luminosity radio galaxies, ~ 30 per cent QSOs and 40 per cent low-luminosity radio galaxies. The expected total number of sources of all kinds at 2 Jy (within the solid angle of 4.05 sr for the 3CR catalogue) is $2380 + 1480 = 3860$, whereas at 10 Jy it was 217. This means that the $\log N - \log F$ slope x , defined by

$$5^x = \frac{217}{3860}, \quad (20)$$

is $x = -1.79$, very close to the values of -1.8 widely quoted in the 1960s, thereby verifying the correctness of the theoretically calculated points of Fig. 3 at $F > \sim 1$ Jy, i.e. at the bright end of the count.¹

The steeper-than-Euclidean slope from 10 Jy down to 2 Jy comes from an excess of $3860 - 217(5)^{3/2} = 1430$ sources which are made available by a penetration from the present half-cycle into the previous oscillatory cycle. That is to say, about 40 per cent of the 4C sources are from the previous oscillatory cycle: 20 per cent radio galaxies and 20 per cent QSOs. The distribution of redshifts for these excess sources is shown by the histogram in Fig. 4, with most of the redshifts being either small or negative. Fig. 4 has been constructed for sources with a standard luminosity of 5×10^{29} W Hz⁻¹, a sufficiently high value to provoke a considerable breakthrough into the previous oscillatory cycle. The curious redshift distribution shown in this figure applies, as has just been remarked, to ~ 40 per cent of sources at the 4C level, the rest being either low-luminosity sources or high-luminosity sources at large redshifts in the present half-cycle like those of 3CR. The abscissa is non-linear in order to show three equal boxes for the redshift ranges $-0.141 \leq z \leq -0.094$, $-0.094 \leq z \leq 0.064$ and $0.064 \leq z \leq 0.419$, which contain equal numbers of sources, while the range $0.419 \leq z \leq 1.174$ contains half the number of the others. There are few sources with $z > 1.174$ from the breakthrough into the previous cycle, most high-redshift

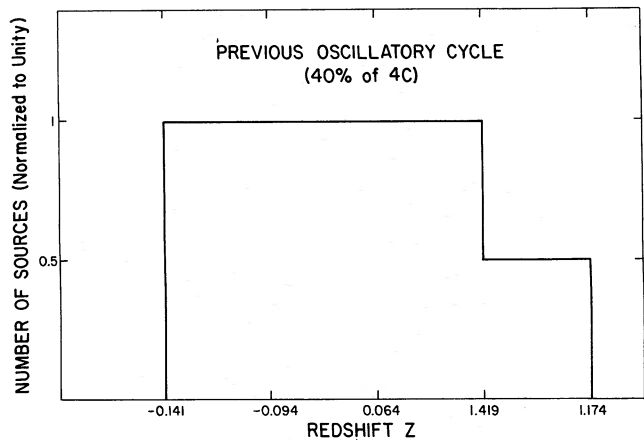


Figure 4. The redshift distribution for the 40 per cent of 4C sources coming from the previous oscillatory cycle, the sources having the high-luminosity value of 5×10^{29} W Hz⁻¹. The non-linear scale for the abscissa has been chosen to show that the redshift bins $-0.141 \leq z \leq -0.094$, $-0.094 \leq z \leq 0.064$ and $0.064 \leq z \leq 0.419$ have equal numbers of sources, while the bin for $0.419 \leq z \leq 1.174$ contains half that number. Partly because sources from the previous cycle are visually faint, and partly because of a lack of suitable emission lines, sources with $z < 0.067$ are likely to be hard to identify (Section 5).

sources in the 4C catalogue being simply the extension of the 3CR sources within the present half-cycle.

What is the present state of identifications for sources with fluxes above 2 Jy? Unlike the situation for sources above 10 Jy, it is very incomplete. Of approximately 2000 sources in the 4C catalogue, about 360 QSOs have been identified and have measured redshifts (Hewitt & Burbidge 1993), and about 260 galaxies with strong emission lines have been identified (Hewitt & Burbidge 1991) and have had redshifts measured. In our view, this minor fraction of identified sources belongs to the present half-cycle. We believe that this is the case because they are comparatively bright in the optical region. Sources from the previous cycle are heavily discriminated against because they should be visually fainter by some 5 mag, as can be seen in Fig. 1. For such faint objects, it would first be necessary to obtain more accurate radio positions than are currently available if identifications were to be attempted. For the majority of the sources in catalogues like the 4C this has simply not been attempted (Condon, private communication). Many radio sources at this level have been designated 'empty fields', meaning that there is nothing brighter than the limit of the optical plates visible. Such 'empty fields' may ultimately turn out to be very faint QSOs, and intrinsically faint galaxies lying at great distances which may have small redshifts or blueshifts if our theory is correct. However, there is a problem with the detection of blueshifts which has still to be considered.

Line radiation at a laboratory wavelength λ_{lab} from an object of redshift z in the previous oscillatory cycle would pass through the last oscillatory minimum with wavelength $\lambda_{\text{lab}}(1+z)/(1+z_{\text{min}})$. Because of the large-scale creation of hydrogen at this epoch, sufficient H I would be expected to be distributed on an extragalactic scale to prevent transmission of the line when

¹ It may be noted that all these numbers assume the flux values in the 3CR catalogue to be correct, whereas it is now known that they are systematically too high (cf. Jauncey 1975). In terms of true flux values, the above numbers of sources per steradian are about 50 per cent too high, ~ 600 sources per steradian rather than 900 at $F = 2$ Jy. For our purpose, it is best to keep to the above numbers and, if a correction is needed, to lower F from 2 Jy down to ~ 1.7 Jy.

$$\lambda_{\text{lab}} \frac{1+z}{1+z_{\text{min}}} < 912 \text{ \AA}, \quad (21)$$

912 Å being the Lyman limit. Of the lines commonly used in redshift determinations, H α (6562 Å) and O III 5007 have the longest wavelengths. To put $\lambda_{\text{lab}} = 5007 \text{ \AA}$ in (21) requires $z > 0.067$. Thus, unless either (i) only H II is present at oscillatory minima, or (ii) emission lines with wavelengths longer than 5340 Å are observed, blueshifts ($z < 0$) will not be found.

Provided that clouds of hydrogen at $t = 0.5$ have densities not less than $10^{-25} \text{ g cm}^{-3}$, recombinations in H II regions with large quantities of hydrogen available proceed rapidly enough to ensure that there is sufficient H I to make (i) inapplicable, while in respect of (ii) no convenient longer wavelength line except H α suggests itself, and of course redshift determinations based solely on H α have never been claimed to be present. The Balmer continuum arising from recombination at the last oscillatory minimum is, however, potentially observable. At time t_0 it will begin in the near-infrared at a wavelength of

$$\frac{0.3646(1+z_{\text{min}})}{1 + \sim 0.44 \overline{kT_e}} \mu\text{m}, \quad (22)$$

where $\overline{kT_e}$ is the average recombining electron energy in electron volts. For $\overline{kT_e} = 1 \text{ eV}$ and $z_{\text{min}} = 4.86$, the resulting present-day infrared continuum would therefore begin at $\sim 1.48 \mu\text{m}$, close to where such a continuum has in fact been found to begin.

To conclude this section, we summarize our predictions for sources above the threshold of the 4C catalogue.

(i) About 40 per cent are low-luminosity radio objects ($L \ll 10^{29} \text{ W Hz}^{-1}$) and are mostly galaxies at moderate redshifts.

(ii) About 20 per cent are high-luminosity objects ($L \geq 10^{29} \text{ W Hz}^{-1}$) like those in the 3CR catalogue with high redshifts.

(iii) About 40 per cent are high-luminosity radio objects from the previous cycle, with low negative or positive redshifts as in Fig. 4, about a half being radio galaxies and half QSOs. The galaxies can be expected to have visual magnitudes of $+24 + \Delta$, i.e. $+25$ for $\Delta = 1 \text{ mag}$, and will simply show as faint fuzz, while the QSOs will have optical magnitudes of about $+20 + \Delta$, i.e. $+21$ for $\Delta = 1 \text{ mag}$.

(iv) Because of absorption at the last oscillatory minimum, values of z of less than about 0.067 will be difficult to measure for sources in (iii), although such measurements, if they could be achieved, would provide an interesting confirmation of the theory.

We emphasize again that the luminosity function of sources has been taken to be the same in each oscillatory cycle, and the same at all phases of a cycle. Some variability from this restrictive condition would be expected, if only from natural fluctuations, and these would be expected to show in the source counts. Thus the theory possesses resources that go a long way beyond those exploited in the above discussion. Without knowing what deviations there might be, however, we have preferred to retain the restrictive assumption of uniformity.

It is perhaps worth emphasizing again that the sources that come from a previous cycle will be much fainter optically than those from the present cycle, and the objects that we have just predicted may exist are not likely to have been found by present techniques which have involved going to weaker radio sources and looking for optical objects. For example, Allington-Smith et al. (1988) identified and measured redshifts for 13 1-Jy radio sources. They identified and measured redshifts for seven galaxies with r magnitudes of 19.5, 20.2, 18.4, 20.8, 23, 23 and 19.5, two QSOs with r magnitudes of 20.5 and 20, and four objects with r magnitudes of 19.5, 20.9, 18.0 and 21.5. The redshifts range from 0.361 to 2.249.

In addition, deep *radio* surveys over very limited regions of the sky at the millijansky level suggest that the majority of the sources are galaxies that are at modest cosmological redshifts ($z \sim 0.5\text{--}0.75$, $m_v = 23$), i.e. a population of intrinsically lower luminosity radio galaxies than those in the 4C catalogue, etc. (Kron, Koo & Windhorst 1985; Windhorst, Dressler & Koo 1987; Windhorst et al. 1993).

6 THE ANGULAR DIAMETER-REDSHIFT RELATION OF RADIO SOURCES

Many years ago, one of us (Hoyle 1959) showed that, if a sufficiently similar sample of radio sources could be observed, their angular diameters plotted against their redshifts could, for redshifts $z \gtrsim 1$, give information that would help to determine the cosmological model. The angular diameter calculation in itself is simple. Putting $dt = dr = d\varphi = 0$ in (1), we obtain

$$d\theta = (1+z) \frac{ds}{r}, \quad (23)$$

in which ds is the proper physical scale of the source in question. Provided that a number of sources with different r -coordinates have the same ds , measurements of $d\theta$ give a relation between z and r ; i.e. we can obtain information on the scale factor $S(t)$.

In the first attempts to use this test to learn about cosmological models, the intrinsically large double radio sources were used with θ given by the separation between the lobes. For Friedmann models with $q_0 = 1/2$ or $+1$, a *minimum* is reached in $d\theta/ds$ at $z \approx 1$. However, the early observations (Wardle & Miley 1974) and those carried out more recently (Kapahi 1987) show strong evidence that $d\theta/ds$ falls off at least as steeply as $1/z$ throughout the range of measurements. To save the conventional picture, it has therefore been necessary to assume either that the component separation decreases with cosmic epoch, or that there is an inverse relation between linear size and radio power so that in a flux-limited sample the smaller and more luminous sources tend to be selected.

Kellermann (1993) has tried this test using extremely compact radio sources. While he has trouble defining the linear part of the plot of θ against z , he finds that, for redshifts > 1 , $d\theta/ds \sim \text{constant}$. At $z \sim 3$ the data lie above the extrapolated $1/z$ law by an order of magnitude. Thus he concludes that this test is compatible with conventional cosmology.

What do we predict within the framework of QSSC?

Let us first make a comparison with Kellermann's result for very small sources. It can be seen from the fourth column of Table 3 that $(1+z)/r$ is nearly constant for $z > 1$, so that our theory is certainly compatible with Kellermann's results.

We believe that the difference between the results from the two different classes of sources is due to the fact that the sources used by Kellermann are wholly intrinsic, whereas on the other hand, for the much larger sources, an interaction with an external medium appears to be involved, an interaction which causes ds to vary with the cosmological scale factor $S(t)$, thus relating ds to z . This changes the dependence of $d\theta$ on z .

Our picture is the following. As described in HBN I, sources arise from creation events in which winds of particles are ejected in bipolar jets, the particles being mainly protons and electrons, the protons having kinetic energies of ~ 1 GeV. Dramatic radio events do not occur until such jets impinge, at considerable distances from their regions of origin, on ambient intergalactic gas. Appreciable slowing of the outward motions of the fast-moving protons results in a complex of electromagnetic processes, of which the production of high-energy electron-positron pairs eventually results in the emission of radio waves. For an appreciable slowing of the protons to occur, the quantity of extragalactic gas, $4\pi\rho_{\text{gas}}(ds)^3/3$ for a region of dimension ds and average gas density ρ_{gas} , must be comparable with the mass of the outward-moving protons. Taking the latter to be the same for all sources of what in the previous section was called the high-luminosity class, the proper length-scale ds on which radio emission largely occurs is seen to be proportional to $\rho_{\text{gas}}^{-1/3}$, with ρ_{gas} likely to be variable according to the phase of the oscillation. Were the total quantity of intergalactic gas to remain independent of time, ρ_{gas} would vary as S^{-3} , and so ds would vary as S , which is to say as $(1+z)^{-1}$. This is possible, but with creation leading to the origin of the gas occurring most strongly at the minima of $S(t)$, and with the ongoing tendency of such gas to condense on to galaxies, some additional dependence of ρ_{gas} on $S(t)$ is to be expected, say an additional linear dependence, giving $\rho_{\text{gas}} \propto S^{-4}$, and so $ds \propto (1+z)^{-4/3}$ and

$$d\theta \propto \frac{1}{r(1+z)^{1/3}}. \quad (24)$$

Table 3. Calculated angular diameters for sources of the same intrinsic proper scale ds .

t	z	r	$\frac{d\theta}{ds} = \frac{1+z}{r}$
.84	.028	.0101	101.8
.82	.094	.0313	34.95
.80	.173	.0539	21.76
.78	.268	.0782	16.21
.76	.382	.1046	13.21
.74	.520	.1334	11.39
.72	.687	.1652	10.21
.70	.890	.2007	9.42
.68	1.135	.2405	8.88
.66	1.432	.2857	8.63
.64	1.790	.3373	8.27
.62	2.216	.3966	8.11
.60	2.710	.4649	7.98
.58	3.261	.5435	7.84

This gives a slightly steeper slope than the Euclidean value, but it does not depart significantly from the observed points of Kapahi (1987).

7 DEDUCTION OF THE SMALL ANISOTROPY AND OF THE TEMPERATURE OF THE MICROWAVE BACKGROUND

In HBN I we were still considering a situation in which the time-scale P was similar to Q . This led to a model with a high creation rate and with extremely massive creation centres, 10^{16} to $10^{17} M_{\odot}$, and it was the degradation of radiation from such centres that was considered to supply the microwave background. In HBN II, however, we showed that with $P \gg Q$ all the pressures that had been exerted on the classical steady-state model were greatly relieved. Moreover, the microwave background could be explained more simply as a consequence of the thermalization of starlight. Thermalization was considered to occur at oscillatory minima in a two-stage process: first an absorption of visible and ultraviolet radiation by carbonaceous grains with re-emission into the infrared, and then a conversion of infrared radiation to microwaves by iron whiskers, the latter occurring with much smaller mean free paths for radiation quanta than the former.

Now, irregularities in the distribution of carbon grains must lead in such a two-stage process to spatial variations, probably on a scale of 10^{25} to 10^{26} cm, in the feeding of energy into the microwave background. However, because the time-scale for the process, $\sim 10^{17}$ s, permits radiation to travel $\sim 3 \times 10^{27}$ cm, there is ample time for regions of high microwave energy density to fill in regions of lower energy density. Such a trend towards homogeneity is not impeded by the opacity of iron whiskers, until deviations from uniformity become very small. The total average proper energy density of the microwaves near oscillatory minima is $\sim 5 \times 10^{-10}$ erg cm^{-3} , and a fluctuation in this value by a small factor x is nevertheless able to move a density ρ_{Fe} of iron whiskers at speed V given by $1/2\rho_{\text{Fe}}V^2 \approx 5 \times 10^{-10}x$. With $\rho_{\text{Fe}} = 10^{-35}$ g cm^{-3} at the present day, the value of ρ_{Fe} at oscillatory minima would be $\sim 2 \times 10^{-33}$ g cm^{-3} , and with $V \approx 0.1c$, an adequate speed to fill in regions of scale 10^{25} to 10^{26} cm in 10^{17} s, the microwave distribution would evidently tend to uniformity despite the inertia of the iron whiskers, provided that x is not less than 2×10^{-5} , i.e. provided that temperature fluctuations in the microwave background are not less than 5×10^{-6} . This then one can see, on simple and straightforward grounds, is the expected fluctuation level of the microwave background, a result agreeing well with the recent COBE results (Smoot et al. 1992).

A scale of 10^{26} cm at oscillatory minima would expand to $\sim 5 \times 10^{26}$ cm at the present day. Regions of such dimensions observed from a medium-range cosmological distance of 5×10^{27} cm would subtend angles of $\sim 5^\circ$ at the observer, again agreeing with the COBE results.

Two of us (Hoyle & Burbidge 1992) have pointed out that there are other more recent possibilities for generating anisotropies in the microwave background, of which the conversion of galactic radiation in the far-infrared by iron whiskers at redshifts typically of ~ 0.3 differs from the above in not having a large measure of absorption and re-emission. This permits irregularities in the whisker distribution to generate fluctuations in the background, unlike the situation

near oscillatory minima where the large degree of absorption and re-emission produces a close approximation to a black-body frequency distribution in which irregularities in the thermalizing agent cannot be distinguished. However, the energy density involved in recent infrared conversion is small, so that the expected anisotropies, which can occur on any angular scale, are again necessarily very weak (Hoyle & Burbidge 1992).

It was shown in HBN II that simple considerations suggest that the background temperature must be close to 2.7 K. We repeat this former calculation, having now arrived from the radio source counts at a better value of the ratio P/Q . Also needed in the calculation is the present-day energy density of intergalactic starlight, which we regard as coming largely from dwarf stars, i.e. from old star populations, typically of spectral type K with a bolometric correction of about 0.75 mag. Thus the usual estimate of $\sim 10^{-14}$ erg cm^{-3} for the energy density in the visual spectrum becomes $\sim 2 \times 10^{-14}$ erg cm^{-3} for the total energy density of starlight.

Averaging over large volumes, write ε for the starlight production rate per unit volume per unit time. With starlight coming from suitably old stars, the production rate ε can be considered as approximately constant over the time-scale Q , i.e. over an oscillatory cycle. Then, with the time t in units of Q , the average production since the last oscillatory minimum is

$$\varepsilon \int_{0.5}^{0.85} \frac{dt}{1+z}. \quad (25)$$

This is per unit coordinate volume, the factor $1/(1+z)$ appearing in the integral because of the redshifting of every quantum. Setting (25) equal to the present-day total energy density of starlight, we determine ε via

$$\varepsilon \int_{0.5}^{0.85} \frac{1+0.75 \cos 2\pi t}{1+0.75 \cos 2\pi t_0} dt = 2 \times 10^{-14}, \quad (26)$$

whence after evaluating the integral we have

$$\varepsilon = 1.14 \times 10^{-13} \text{ erg cm}^{-3} \text{ per unit time}, \quad (27)$$

with unit time being Q . Thus the total production of starlight from the previous oscillatory minimum at $t = -0.5$ to that at $t = 0.5$ is

$$\varepsilon \int_{-0.5}^{0.5} \frac{dt}{1+z} = 4.56 \times 10^{-13} \text{ erg cm}^{-3}, \quad (28)$$

(27) being used for ε .

Now the weakening in such a cycle of the energy density, W_{\min} say, at oscillatory minima of the microwave background due to the factor $\exp(t/P)$ in $S(t)$ is $4QW_{\min}/P$, and, to maintain the background from cycle to cycle at a steady level, the input (28) arising from the thermalization of starlight must just compensate this loss rate. Thus the steady requirement for $P/Q = 20$ gives

$$W_{\min} = 1.14 \times 10^{-13} \frac{P}{Q} = 2.28 \times 10^{-12} \text{ erg} \\ \text{per unit coordinate volume in cm}^{-3}. \quad (29)$$

Since (29) is with respect to coordinate volume, there is a weakening of the background energy density by $S(0.5)/S(t_0)$ between the last oscillatory minimum and the present time $t_0 = 0.85$, i.e. by a factor 0.1734 to

$$W_{\text{present}} = 3.96 \times 10^{-13} \text{ erg cm}^{-3}. \quad (30)$$

The cosmological scale factor being adjusted to be unity at $t = t_0$, this is also the present-day energy density of the microwave background per unit proper volume. Dividing (30) by the radiation density constant and then taking the fourth root, we obtain

$$T_{\text{CMB}} = 2.68 \text{ K}, \quad (31)$$

very close to the observed value of 2.73 K.

8 THE PROPERTIES OF IRON WHISKERS AND THEIR ASTROPHYSICAL CONSEQUENCES

Wickramasinghe & Hoyle (1994) have recently improved on their earlier calculations of the opacity of iron whiskers (Hoyle & Wickramasinghe 1988; Wickramasinghe, Wickramasinghe & Hoyle 1992). By using the Drude theory of metals together with the earlier work, it has been shown how the mass absorption coefficient $\kappa(\lambda)$ can be obtained for any specified ratio of the whisker length l to its radius a , using only the measured cryogenic d.c. conductivity of iron, $6.9 \times 10^{18} \text{ s}^{-1}$ according to the American Institute of Physics Handbook. Since the calculations depend on the whisker dimensions only as l/a , it is sufficient to standardize a and to present results for various values of l . This has been done in Table 4, from which the function $\kappa(\lambda)$ can be constructed for any assigned value of l or a mixture of values of l . Thus Fig. 5

Table 4. Results for a d.c. conductivity of $6.90 \times 10^{18} \text{ s}^{-1}$ and a whisker diameter of $0.02 \mu\text{m}$.

WL(MU)	Mass Absorption Coefficient ($\text{cm}^2 \text{g}^{-1}$)					
	LENGTH =					
	1000	500	300	200	100	$50 \mu\text{m}$
1.00E0	1.86E3	1.86E3	1.86E3	1.86E3	1.86E3	1.86E3
2.00E0	5.00E3	5.00E3	5.00E3	5.00E3	5.00E3	5.00E3
3.00E0	9.24E3	9.24E3	9.24E3	9.24E3	9.24E3	9.24E3
5.00E0	2.04E4	2.04E4	2.04E4	2.04E4	2.04E4	2.04E4
1.00E1	6.00E4	6.00E4	6.00E4	6.00E4	6.00E4	6.00E4
2.00E1	1.72E5	1.72E5	1.72E5	1.72E5	1.72E5	1.72E5
3.00E1	3.19E5	3.19E5	3.19E5	3.19E5	3.19E5	3.19E5
5.00E1	7.12E5	7.12E5	7.12E5	7.12E5	7.12E5	7.12E5
1.00E2	2.21E6	2.21E6	2.21E6	2.21E6	2.21E6	2.21E6
2.00E2	6.89E6	6.89E6	6.89E6	6.89E6	6.89E6	1.01E6
3.00E2	1.30E7	1.30E7	1.30E7	1.30E7	5.81E6	4.49E5
5.00E2	2.68E7	2.68E7	2.68E7	2.42E7	2.14E6	1.62E5
1.00E3	5.73E7	5.73E7	2.73E7	6.99E6	5.39E5	4.04E4
2.00E3	8.88E7	3.96E7	8.11E6	1.82E6	1.35E5	1.01E4
3.00E3	8.54E7	2.13E7	3.73E6	8.14E5	6.00E4	4.49E3
5.00E3	5.50E7	8.63E6	1.37E6	2.94E5	2.16E4	1.62E3
1.00E4	2.06E7	2.27E6	3.45E5	7.37E4	5.40E3	4.04E2
2.00E4	5.89E6	5.76E5	8.65E4	1.84E4	1.35E3	1.01E2
3.00E4	2.69E6	2.57E5	3.84E4	8.19E3	6.00E2	4.49E1
5.00E4	9.81E5	9.26E4	1.38E4	2.95E3	2.16E2	1.62E1
1.00E5	2.47E5	2.32E4	3.46E3	7.37E2	5.40E1	4.04E0

Note: 1.00E1 = 1.00×10^1 .

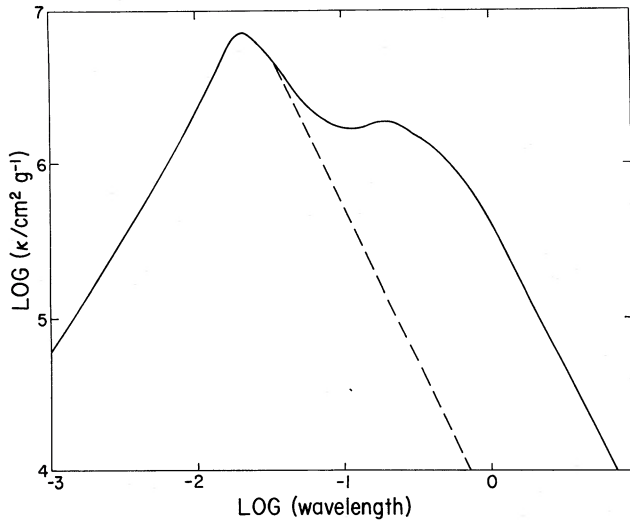


Figure 5. A plot of mass absorption coefficient for iron whiskers of radius $a = 10^{-2} \mu\text{m}$ and lengths $l = 100$ and $1000 \mu\text{m}$ in a ratio by mass of 50:1. The broken curve shows what $l = 100 \mu\text{m}$ alone would give. The abscissa scale is centimetres (Section 8).

gives $\kappa(\lambda)$ for a mixture of whiskers with lengths $l = 100$ and $1000 \mu\text{m}$ in a mass ratio of 50 to 1. The broad maximum defined by $\kappa \geq 10^6 \text{ cm}^2 \text{ g}^{-1}$ extends from $\lambda = 60$ to $500 \mu\text{m}$, in the rest frame of the whiskers. With the microwaves produced at redshifts close to $z_{\text{min}} = 4.86$, the broad maximum of Fig. 5 covers the wavelength range at observation from $\lambda = 0.35$ to 3 mm , just the range containing the bulk of the energy of the microwave background.

The discussion of the radio source counts in Sections 4 and 5 assumed implicitly that at the frequencies discussed there, 408 MHz and 1.4 GHz, the observed fluxes were not affected significantly by absorption, even for sources from k oscillatory cycles ago, with k determined by

$$\exp(-6kP/Q) \approx 0.1, \text{ i.e. } k = 8 \text{ for } P/Q = 20.$$

Writing τ for the optical depth at each oscillatory minimum for frequency 1.4 GHz, this condition implies that $k\tau \leq \sim 1$, which for $k = 8$ requires that $\tau \leq 0.125$. Now, a frequency of 1.4 GHz at observation was a frequency of 8.2 GHz at the last oscillatory minimum, i.e. $\lambda = 3.7 \text{ cm}$, where according to Fig. 5 the mass absorption coefficient $\kappa(\lambda)$ is less than its value in the broad maximum responsible for the main energy distribution of the microwaves, by a factor of $\sim 10^{-2}$. Hence for an optical depth of ~ 10 at each oscillatory minimum, taken for the main energy distribution of the microwaves, the corresponding optical depth for radio waves at $\lambda \approx 3.7 \text{ cm}$ (observed today at 1.4 GHz) is ~ 0.1 per oscillatory cycle, an allowable value. Because of the steep fall of the curve of Fig. 5 to longer wavelengths, absorption at 408 MHz would be negligible. By the same token, absorption would be more significant at frequencies above 1.4 GHz. Source counts at higher frequencies, however, are not required to penetrate through $k \approx 8$ cycles, since the higher frequency surveys appear to be concerned only with low values of k . Indeed, for the higher frequency of 5 GHz, only the present half-cycle back to $z_{\text{min}} = 4.86$ appears to be involved in the counts.

It is of interest to estimate the background temperature T produced at 1.4 GHz by the iron whiskers. This is deter-

mined in a steady-state situation by the equation

$$\tau T_{\text{CMB}} - f \frac{Q}{P} T - \tau T = 0, \quad (32)$$

where T_{CMB} is the main microwave background temperature of 2.73 K, this being the temperature of the whiskers. The first term on the left-hand side of this equation is the increment at 1.4 GHz for each oscillatory cycle, the second is the decrement of temperature due to the expansion of the Universe, and the third term is the decrement per cycle due to self-absorption by the whiskers. Because τ is frequency-dependent, so also is the solution T of equation (32). It is this that introduces the factor f in (32). We estimate about 2/3 for f , when at 1.4 GHz we get $T = 2.155 \text{ K}$ for $\tau = 0.125$ and $T_{\text{CMB}} = 2.73 \text{ K}$. Measurement of the background temperature at 1.47 GHz by Bensadoun et al. (1993) gave $2.27 \pm 0.19 \text{ K}$.

A referee has raised the question whether absorption in the broad peak of Fig. 5 would produce too much absorption in microwave CO lines found in the extremely luminous infrared galaxy IRAS 10214+4724 (Solomon, Downes & Radford 1992). It is not hard to show that the line-of-sight opacity to an object of high redshift z is approximately proportional to $(1+z)^3$. Taking the microwave opacity at $z_{\text{min}} = 4.86$ to be 5 (half the above value of 10, which was for the double-sided path through the last oscillatory minimum into the previous cycle), the optical depth to IRAS 10214+4724 with $z = 2.286$ would be $\sim 5(3.286/5.86)^3 = 0.88$. To compensate for an absorption factor $\exp(-0.88)$, the intrinsic CO line emissions of IRAS 10214+4724 would need to be increased by a factor of about 2, but we see no reason why this may not be the case. Even if molecular lines were eventually detected from an object with $z \approx 4$, the increase of the intrinsic emissions required to compensate for absorption would not be particularly relevant, since we have no datum that sets an upper limit to the intrinsic emissions required.

In a recent progress report, Isaak et al. (1993) have discussed fluxes obtained with the James Clerk Maxwell Telescope from a QSO with redshift $z = 4.7$. A spectrum is shown with a high peak at $\sim 500 \mu\text{m}$ and wings going from ~ 100 to $\sim 5000 \mu\text{m}$, the observations being in three bands on the immediate long-wavelength side of the peak. The short-wavelength side is consistent with a redshifted Planck spectrum having a temperature of $\sim 40 \text{ K}$ at source. The long-wavelength side, however, falls much more rapidly than a Planck distribution of this temperature would do, suggesting the possibility that the observed steep longward fall may be due to whisker absorption from the broad maximum of Fig. 5, a situation similar to that found in our own Galaxy by Wickramasinghe & Okuda (1994) for the absorption of the C II 157- μm and N II 205- μm lines.

We have indicated already that a good approximation to isotropy is to be expected in the distribution of microwaves. We emphasize this point again. The first step, whereby radiation in the visual and near-infrared is degraded by ordinary dust into the farther infrared, already introduces a considerable degree of isotropy. Thus an ordinary intergalactic dust particle normally receives most radiation from distant galaxies approximately isotropically distributed, this being the well-known Olbers effect. Only within a few hundred kpc

of galaxies is there any dominant local effect, and this applies only to a small fraction of the extragalactic volume. Thus the conversion to the farther infrared is mainly smooth, but with local islands of higher energy density in the immediate neighbourhood of galaxies. In the conversion to microwaves by iron whiskers, then, these local islands are removed essentially by the factor $\exp(-\text{optical depth})$, and with an optical depth of ~ 10 per cycle the remaining irregularities are of the order of 1 part in 10^4 of the injection per cycle, or, since the injection per cycle is of the order of one-tenth of the total microwave energy, irregularities in the injection are of the order of 1 part in 10^5 of the total, in agreement with the estimate obtained above from an explicit consideration of the dynamical process whereby smoothing of the local islands occurs. It remains to note that irregularities do not accumulate from cycle to cycle, for the important reason that the microwaves travel and mix over great distances, 10^{28} to 10^{29} cm, at phases near oscillatory maxima.

9 DISCUSSION AND CONCLUSION

A number of issues discussed in the previous section depend on the explicit form of Fig. 5. A satisfactory resolution of the issues in question depends on the choices of the conductivity and the length-to-diameter ratio for iron whiskers. Other choices might be made that would cause more difficulty for the theory, a circumstance that we do not deny. On the other hand, a more complicated model involving a spread in the properties of whiskers might be considered, and, as more complicated models usually have a greater resilience in fitting observational constraints, the theory might well be improved.

We think that the reader will not fail to be impressed by the degree of astrophysical detail that can be brought into the range of discussion by using this theory.

The theory seeks to demonstrate that every observable property of the Universe is self-maintaining, an idea taken over from the classical steady-state theory of 1948. In addition, the initial data used are themselves derived directly from observation, so far as is possible. Thus the need for the entire Universe to originate is avoided, and in principle the need for arbitrariness in the initial data is also avoided. The manner of obtaining the temperature of the microwave background in Section 7 illustrates this procedure. We accept that at the present time the situation is not as secure as we would like it to be, as for example in respect of the existence of iron whiskers in extragalactic space, an essential component of our argument. However, what can be said is the following. When metallic vapours are cooled slowly enough in the laboratory, whiskers are formed by a well-understood process which one can expect to operate during the cooling of metallic vapours in the expansion of the envelopes of supernovae. The escape of such particles from galaxies into extragalactic space is also to be expected, because of the strong radiation pressure to which they are subjected by sources in the far-infrared, strong sources which are known to exist widely in galaxies. Thus the logical steps for supposing that whiskers exist in intergalactic space are clear-cut. Of course, we would prefer to have direct observational evidence of their presence, and this may eventually be forthcoming. At present there is growing, but still tentative, evidence of the existence of discrete microwave sources and these may turn

out to supply the direct evidence, illustrating the on-going nature of the present theory, which in its nature is capable of improvement and change as more evidence comes to light and as new concepts suggest themselves. Our situation is not locked into an arbitrary parameter-fitting format, as is the case with the big bang.

In the big bang cosmology, it is argued that the synthesis of D, ^3He , ^4He and ^7Li in the early Universe is a matter of deduction and not accommodation, and this has a claim to respectability. Within the framework of this theory, however, something of a tightrope balancing act with the baryon-to-photon ratio is necessary even to get the abundances of only four nuclides in reasonable correspondence with observation. It is also the case that, in the abundance tables, the three elements Li, Be and B form a tight group quite apart from the rest, strongly suggesting a common origin. Big bang nucleosynthesis, however, does not produce either Be or B, or at any rate not without considerable deviations from the canonical position. Thus a different mode of origin for Be and B is needed, usually cosmic ray spallation on ^{12}C and ^{16}O , which just happens coincidentally to yield similar abundances to the primordial genesis of ^7Li . Regarding ^7Li , also, primordial synthesis is considered to explain the low abundances found in Population II stars, while the significantly higher abundances of lithium in some Population I stars come, it is supposed, from an astrophysical process of origin. So for ^7Li there are again two processes, one cosmological and the other taking place in stars.

What the big bang has in common with the present theory is that, in the present theory, matter begins as Planck particles which decay in fireballs to large numbers of baryons, the physical conditions in the fireballs yielding a form of primordial nucleosynthesis (Hoyle 1992; HBN I, appendix), a form which includes the synthesis of Be and B, and of ^6Li as well as ^7Li . More knowledge is needed before entirely parameter-free calculations of this process can be made. However, the correct abundances for D, ^3He and ^4He are obtained in calculations that are essentially parameter-free, while correct abundances for all the isotopes of Li, Be and B require only the adjustment of a single parameter determining the intensity of the radiation field coming from quark transitions within the fireballs.

The proof from the theory of matter creation discussed in HBN I that matter originates as Planck particles, taken together with the known existence in the laboratory of iron whiskers with the absorption properties shown in Fig. 5, removes the need for a big bang beginning. The basis of our own views lies in the coupling of a scalar field, the so-called C-field, to matter. The coupling can be formulated so as to achieve two things. The C-field provides a negative pressure on which the Universe is able to bounce at the minima of the oscillations discussed above, and it permits matter to be created to a moderate degree at each such minimum, as well as to a smaller degree in every process associated with high-energy astrophysics, ranging down to modest outbursts in ordinary galaxies such as our own. We accept that more knowledge is needed about all these processes, which we consider to lead to a scale function for the Universe of the form of (2). From there on, we believe that the theory must be close to being correct, our reason being the many observational results that are explained without any substantial further adjustment being needed, when the parameters in (2)

have been decided as in (3). Subsequent hypotheses have been simply those of uniformity, such as, for instance, that all radio sources of the high-luminosity class are intrinsically similar to each other, or that the energy density of the microwave background is steadily maintained. The list of observational correspondences is long and, we hope, convincing, and we conclude by summarizing the situation as follows.

(1) In our theory the observational value of the Hubble constant is not in conflict with any form of age estimate, whether of old stars or of the r -process elements. The parameter values in (3) were chosen to give a Hubble constant of about $65 \text{ km s}^{-1} \text{ Mpc}^{-1}$, intermediate between the high and low groups of believers. Small adjustments would take H_0 either down to a low value of $50 \text{ km s}^{-1} \text{ Mpc}^{-1}$ or up to a high value of $80 \text{ km s}^{-1} \text{ Mpc}^{-1}$. By taking observed globular clusters to have formed at the last oscillatory minimum, an age of $14 \times 10^9 \text{ yr}$ for the cluster stars was obtained, subject to the choices of the parameters in (3).

(2) Observation to the last oscillatory minimum leads to a largest value of the redshift z , short of going back to the previous oscillatory minima. This maximum redshift depends only on α and t_0 , not on Q . On the other hand, the Hubble constant and the ages of the globular cluster stars depend largely on Q . The combination of α and t_0 in (3) gives a maximum redshift of 4.76 from the last oscillatory minimum [ignoring the slowly varying factor $\exp(t/P)$ which, if included, increases the maximum redshift to 4.86]. In effect, the Hubble constant, the age of the globular clusters and the maximum redshift determine α , t_0 and Q . Apart from P , the theory is then parameter-free.

(3) For redshifts up to unity, the redshift–magnitude diagram for intrinsically similar galaxies is like that for the Friedmann model with $q_0 = +1$. At larger redshifts, however, galaxies become fainter than in the Friedmann model, especially with absorption occurring near the last oscillatory minimum. An intrinsically very bright galaxy would be observed, if at the last oscillatory minimum, with magnitude $+26$ to $+27$. Penetrating through the last oscillatory minimum towards the maximum of the previous half-cycle, galaxies then have only small redshifts and are consequently blue in colour. The theory thus predicts the existence of a large number of faint blue galaxies of small redshifts.

(4) The mean universal density at oscillatory minima is $\sim 2 \times 10^{-27} \text{ g cm}^{-3}$, which sets a lower limit to the mean density in bound clusters of galaxies, which otherwise at oscillatory minima would become like holes in Swiss cheese.

(5) The conditions at oscillatory minima are highly favourable to the formation of galaxies, which grow bit by bit from one minimum to another. Fully formed galaxies like our own are of an age of order $P/3$, not Q . Star clusters, except those formed at the last oscillatory minimum, have by now been burned down to such low stellar masses that they are no longer individually distinguishable if at any appreciable distance, and so are not available generally for obtaining age estimates. It is these very old stars of low mass that provide the so-called missing mass in galaxies, as is discussed in detail in HBN II.

(6) On the time-scale $P/3$, clusters of galaxies can evolve dynamically to a remarkable degree. Starting as a relatively widely spaced group of largely spiral galaxies, the system evolves through escaping members leading to a tightening

core, where galaxies of elliptical type grow either by repeated condensation of discs of varying orientations forming on top of each other or through mergers, the two processes having very similar effects. Central cluster cores of exceptionally large mass also form, as may well be the situation for cD galaxies. All these processes become credible on the time-scale $P/3$, but they are not credible, it seems to us, on a time-scale of only 10^{10} yr .

(7) The long time-scale of order $P/3$ associated with the process of formation of elliptical galaxies explains the very high mass-to-light ratios, of the order of 100, for these galaxies found observationally. In addition, the general debris accumulating in clusters of great age explains the missing mass in such clusters, the so-called missing mass being in the form of exceedingly faint stars with masses of $\sim 0.1 M_\odot$. The demise of primordial nucleosynthesis (required in the big bang) in favour of nucleosynthesis in Planck fireballs (HBN I) permits ‘missing mass’ to be baryonic.

(8) On the uniformity hypothesis that highly luminous radio sources are similar to one another – such uniformity hypotheses are usually referred to as ‘principles’ – the count of radio sources from the so-called Euclidean level at flux values of order 1 Jy down to low flux values is in good agreement with the theory for $P \approx 20Q$.

(9) The theory explains the steeper-than-Euclidean rise in radio source counts at high flux values, the feature that generated controversy in the 1950s and 1960s.

(10) In our view, radio sources of high luminosity depend on internally expelled material impinging on an external target. While we regard the sources as intrinsically similar to each other, the external target material is related to the phase of the oscillatory cycles. On what seems a reasonable hypothesis concerning this relationship, we can understand the results for the angular diameters of the large double sources. On the other hand, for sources of much smaller angular size, which seem to be wholly intrinsic, the theory predicts an initial decline proportional to the reciprocal of the redshift but tending for $z \geq 1$ to an essentially constant angular diameter, in agreement with the recent results of Kellermann (1993).

(11) The microwave background is the outcome of the thermalization of starlight from the last $\sim P/3$ cycles of the Universe. Because of the large distances travelled by the radiation at oscillatory maxima, and because of the strong thermalization which occurs at each minimum, there is no accumulation of anisotropies from cycle to cycle. Only that from the last minimum survives, and this can be seen to give a temperature fluctuation of $\Delta T/T \approx 5 \times 10^{-6}$.

(12) Subject to a small measure of uncertainty concerning the production of starlight by galaxies, the ratio $P/Q = 20$ leads to a microwave background temperature close to 2.7 K.

These many correspondences with observation seem to us to justify our optimism in regarding the form (2) for the scale factor of the Universe as being close to correct.

ACKNOWLEDGMENTS

We thank D. Duari for help with the computations, and Dr P. Solomon for information concerning sources of CO emission.

REFERENCES

- Allington-Smith J., Spinrad H., Djorgovski S., Liebert J., 1988, *MNRAS*, 234, 1091
- Bensadoun M., Bersonelli M., DeAmici E., Kogut A., Levin S. M., Limon M., Smoot G. F., Witesky C., 1993, *ApJ*, 409, 1
- Clayton D., 1988, *MNRAS*, 234, 1
- Cowan J., Thielemann F.-K., Truran J., 1991, *ARA&A*, 29, 447
- Fowler W. A., 1987, *QJRAS*, 28, 87
- Fowler W. A., Hoyle F., 1960, *Ann. Phys.*, 10, 28
- Hewitt A., Burbidge G., 1991, *ApJS*, 75, 297
- Hewitt A., Burbidge G., 1993, *ApJS*, 87, 451
- Hoyle F., 1959, in Jauncey D. L., ed., *Proc. IAU Symp. 74, Radio Astronomy & Cosmology*. Reidel, Dordrecht, p. 119
- Hoyle F., 1968, *Proc. R. Soc. London, Ser. A*, 308, 1
- Hoyle F., 1992, *Ap&SS*, 198, 177
- Hoyle F., Burbidge G., 1992, *ApJ*, 399, L9
- Hoyle F., Wickramasinghe N. C., 1988, *AP&SS*, 147, 245
- Hoyle F., Burbidge G., Narlikar J. V., 1993, *ApJ*, 410, 437 (HBN I)
- Hoyle F., Burbidge G., Narlikar J. V., 1994, submitted (HBN II)
- Isaak K., Hills R., Withington S., McMahon R., 1993, *JCMT Newsletter*, No. 1, July, p. 38
- Jauncey D. L., 1975, *Rev. Astron. Astrophys.*, 13, 26
- Kapahi V. K., 1987, in Hewitt A., Burbidge G., Fang L.-Z., eds, *Proc. IAU Symp. 124, Observational Cosmology*. Reidel, Dordrecht, p. 251
- Kellermann K., 1993, *Nat*, 361, 134
- Kellermann K., Wall J. V., 1987, in Hewitt A., Burbidge G., Fang L.-Z., eds, *Proc. IAU Symp. 124, Observational Cosmology*. Reidel, Dordrecht, p. 545
- Kristian J., Sandage A. R., Westphal J. A., 1978, *ApJ*, 221, 383
- Kron R., Koo D., Windhorst R., 1985, *A&A*, 146, 38
- Smoot G. F. et al., 1992, *ApJ*, 396, L1
- Solomon P. M., Downes D., Radford S. J., 1992, *ApJ*, 398, L29
- Wardle J. F., Miley G., 1974, *A&A*, 30, 345
- Wickramasinghe N. C., Hoyle F., 1994, *Ap&SS*, in press
- Wickramasinghe N. C., Okuda H., 1994, *Ap&SS*, in press
- Wickramasinghe N. C., Wickramasinghe A. N., Hoyle F., 1992, *Ap&SS*, 193, 141
- Windhorst R., Dressler A., Koo D., 1987, in Hewitt A., Burbidge G., Fang L.-Z., eds, *Proc. IAU Symp. 124, Observational Cosmology*. Reidel, Dordrecht, p. 473
- Windhorst R., Fomalont E., Partridge B., Lowenthal J., 1993, *ApJ*, 410, 498

APPENDIX A: METHOD OF COMPUTER CALCULATION OF THE RADIO SOURCE CURVE (SECTION 4)

Compute by interpolation in tables like Tables 1 and 2 the values of t , r and $1+z$ at which

$$\frac{L}{F} = 4\pi r^2 (1+z)^2 \quad (\text{A1})$$

for an assigned L and F . Suppose that equation (A1) is satisfied for $t_1 > t_2 > t_3 > t_4 > t_5 \dots$ up to an odd multiple of t -values. Then compute the volumes

$$V(t_r) = \int_{t_r}^{t_0} 4\pi r^2 (1+z) \exp \frac{3(t-t_0)}{P/Q} dt, \quad (\text{A2})$$

thus obtaining $N(>F)$ for the relative number of sources brighter than F from the alternating series

$$V(t_1) - V(t_2) + V(t_3) - \dots \quad (\text{A3})$$

Carry out this procedure for $F_1 > F_2 > F_3 \dots$ in some assigned flux range, e.g. 10^{-2} to 10^2 Jy, and calculate the quantities

$$\frac{N(F_n) - N(F_{n-1})}{F_{n-1} - F_n} F_n^{5/2}. \quad (\text{A4})$$

Then, in the luminosity range from 10^{29} to 10^{30} WHZ^{-1} , choose values of L at equal logarithmic intervals and for each one carry out sums as above. Finally, multiply by $L^{-2.1}$ and add the values of (A4) for all the chosen values of L .